

Atomic-Level Description of Amyloid  $\beta$ -Dimer FormationS. Gnanakaran,<sup>†</sup> Ruth Nussinov,<sup>‡,§</sup> and Angel E. Garcia<sup>\*,†</sup>

Los Alamos National Laboratory, T-10, MS K710, Los Alamos, New Mexico 87545, SAIC, Laboratory of Experimental and Computational Biology, NCI-Frederick, Maryland, 21702, Department of Human Genetics, Tel Aviv University, Tel Aviv 69978, Israel, and Department of Physics, Applied Physics, and Astronomy, Rensselaer Polytechnic Institute, Troy, New York 12180

Received July 19, 2005; E-mail: angel@rpi.edu

We provide an atomistic-level description of the organizational and structural ordering and the thermodynamics of oligomerization of dimer formation. It is motivated by the recent clinical studies that have suggested oligomers as the possible pathological agents in Alzheimer's disease.<sup>1–3</sup> Even though dimer is not the critical oligomer, it is certainly an important intermediate. Additionally, a thorough understanding of dimer formation provides a detailed picture of forces that drive the interaction between fragments. Replica exchange molecular dynamics (REMD) is carried out for the 16–22 sequence of the 42-residue  $A\beta$  peptide,<sup>4</sup>  $A\beta_{16–22}$ , in explicit solvent at 38 different temperatures ( $T$ ). The important findings from this work are that (i) the dominant monomer conformation is polyproline II (PP<sub>II</sub>)-like, (ii) the strands are not required to adopt extended conformation to form dimers at low  $T$ , (iii)  $A\beta_{16–22}$  can form at least six different stable dimers and is not necessarily limited to only parallel and antiparallel orientations, (iv) these dimer conformations show a strong  $T$  dependence, (v) the preferential shift in dimer conformations with  $T$  is a result of different kinds of forces driving their formations, and (vi) water molecules are directly involved in stabilizing certain dimer conformations that cannot be predicted from implicit solvent models.

The choice of this short peptide sequence is based on its medical significance and on past experimental and simulation studies.<sup>5–14</sup> Biochemical mutational studies indicate this region as critical for aggregate formation.<sup>5,15,16</sup> The  $A\beta_{16–22}$  is also the shortest fragment from  $A\beta$  for which experimental evidence of amyloid formation is available.<sup>6</sup> Solid-state NMR showed that this segment can form fibrils with the antiparallel strand organization.<sup>7</sup> The sequence of this segment is highly prone to aggregation, a prototype for the process of amyloidosis.<sup>17</sup>

The theoretical challenge is to capture the relevant configurational ensembles of the  $A\beta_{16–22}$  dimers at an atomic level as a function of  $T$  in explicit aqueous solution. The REMD methodology<sup>18,19</sup> was shown to be an effective technique to sample the conformational space of short peptides in explicit solvent. It offers a much-improved approach to determining the oligomer distributions relevant to aggregation.<sup>20–22</sup> REMD was implemented with a constant volume and a fixed number of atoms.<sup>22</sup> Capped  $A\beta_{16–22}$  with the sequence of Ace-KLVFFAE-NH<sub>2</sub> was considered with a modified version of the AMBER94 force field.<sup>23</sup> The monomer was solvated in 1583 water molecules and simulated with 24 replicas covering the  $T$  range of 276–469 K. The dimer was solvated in 1626 waters and simulated with 38 replicas at a  $T$  range of 275–510 K. Replicas maintained an exchange rate of 8–20%. Periodic boundary conditions were applied, and the monomer and the dimer were solvated with TIP3P<sup>24</sup> waters and no counterions in a cubic box with lengths

of 36.7 and 37.7 Å, respectively. The system was coupled to an external heat bath with a relaxation time of 0.1 ps.<sup>25</sup> The generalized reaction field treatment was used for electrostatic interactions with a cutoff of 8 Å.<sup>26</sup> All replicas were started from random conformations. The monomer simulations were performed for 15 ns/replica. The last 10 ns were used in the analysis. Dimer simulations were performed for ~11.5 ns, with the last 6 ns used for analysis.

First we capture different dimer ensembles that are sampled at 310 K. By choosing an appropriate set of order parameters, a free energy landscape that captures most of the relevant dimer conformations is obtained. Figure 1A shows this free energy map as a function of the cosine of the angle between strands and the number of backbone C $\alpha$  contacts (<6.5 Å). At least six distinct basins are seen that correspond to the following stable dimer conformations: shifted parallel strand and parallel loop, parallel strand, antiparallel strand, shifted antiparallel, cross, and tight cross/lock. Completely water-mediated dimers are not considered in this contact-based analysis. These dimers show distinct  $T$  dependencies, reflecting the fact that they are stabilized to different degrees of hydrophobic and polar interactions. Figure 1B shows the changes in the population of different dimers as function of  $T$ . At low  $T$ , the parallel loop and shifted parallel structures are favored. As  $T$  increases, the preference shifts to the antiparallel conformations with shifted dimers dominating at 400 K. Dimers diminish rapidly at high  $T$  where entropy dominates. At ~350 K, strands interlock to provide a large number of backbone contacts. The population of cross conformations (with strands perpendicular to each other) is independent of  $T$ .

The rationale for different  $T$ -dependence of dimers can be explained according to the nature of the interactions driving their formation. Figure 2 provides a residue-level contact map for both backbone–backbone and side chain–side chain interactions at two different  $T$ . At 275 K, the backbone contacts between residues at both terminals drive the formation of parallel loop dimers where the side chains at the C-terminus strongly interact with each other. A water network connects the charged Glu side chains between the strands and stabilizes this conformation. The observation of this conformation is indicative of the importance of explicit solvent and may explain why such conformations were not found in earlier simulation studies using implicit solvent models.<sup>10–14</sup> The side chain contact profile at 275 K also reflects interactions between Val and Ala residues that drive the formation of shifted-parallel dimers. As  $T$  increases (310 K), however, the preference shifts to anti-parallel dimers where the backbone contacts from the middle of the fragments drive the dimer formation. A strong hydrophobic interaction between the side chains of Phe is seen. The interaction between Phe and the N-terminus is indicative of the shifted antiparallel dimers. These conformations are preferred because the

<sup>†</sup> Los Alamos National Laboratory.<sup>‡</sup> NCI-Frederick.<sup>§</sup> Tel Aviv University.<sup>†</sup> Rensselaer Polytechnic Institute.

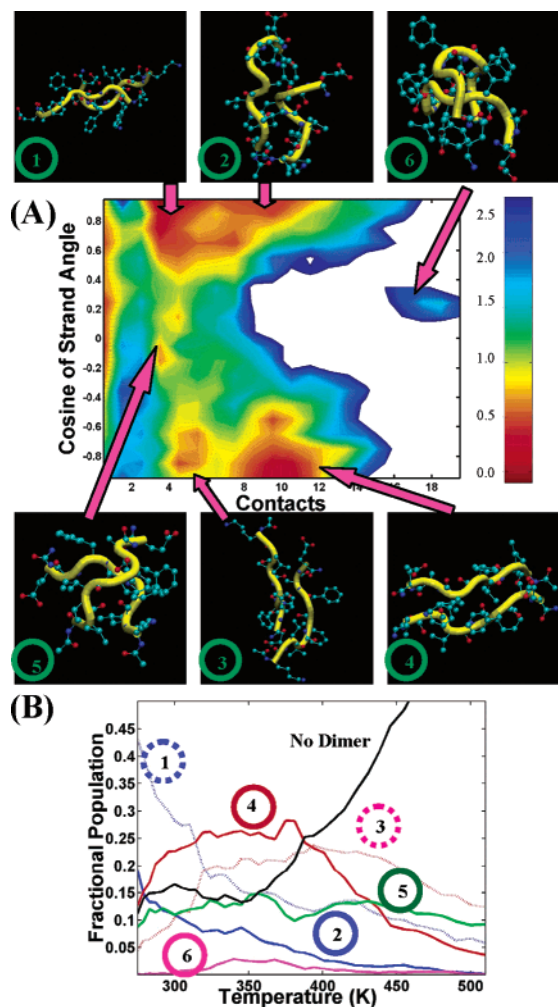


**Figure 1.** (A) Free energy landscape of  $A\beta_{16-22}$  dimers at 310 K. It is plotted as a function of cosine of angle between the strands and the number of contacts between backbone c- $\alpha$  atoms. Representative dimer conformations are shown. (B) T-profile of dimers identified in A.

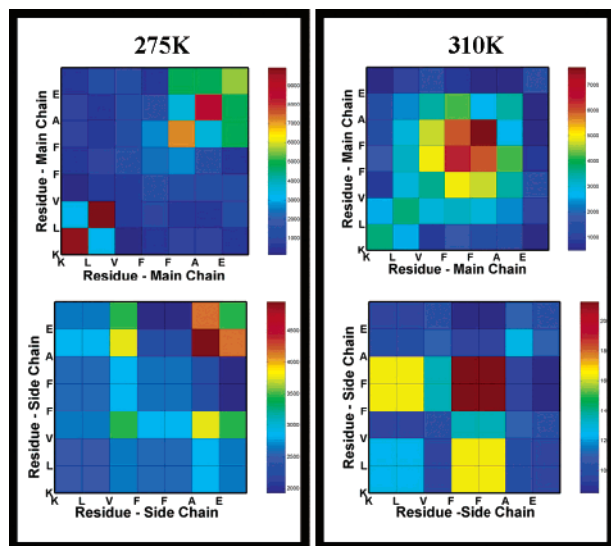


**Figure 2.** Backbone-backbone and side chain-side chain residue contact maps at 275 and 310 K. The color gradient from blue to red is indicative of increase in contacts.

charged Lys at the N-terminus is capable of forming hydrophobic interactions compared to that of the Glu at the C-terminus.

Finally, we explore how the secondary structural propensity of the monomer is perturbed as the fragments form dimers (Supporting Information). In the simulations of solvated monomer,  $A\beta_{16-22}$  predominantly adopts  $PP_{II}$  structure. The 40%  $PP_{II}$  content obtained from the simulations is close to values obtained in measurements on the 1–28 segment of the  $A\beta$ .<sup>27</sup> In the dimer simulations, when two fragments associate to form a dimer at low  $T$ , the monomer neither adopts the  $\beta$  structure as in fibrils nor exhibits any other secondary structure preference. However, as  $T$  increases, they prefer extended conformations.

In summary, this all-atom simulation study reveals that dimers of the aggregation-prone fragment of  $A\beta$  peptide do not necessarily adopt only parallel and antiparallel conformations commonly seen in the amyloid fibril.

**Acknowledgment.** We thank B. Ma for help in starting this project. This project has been funded in whole or in part with funds from the NCI-NIH (contract No. NO1-CO-12400), National Science Grant DMR-0117792 and LDRD (Los Alamos).

**Supporting Information Available:** Supporting Figure. This material is available free of charge via the Internet at <http://pubs.acs.org>.

## References

- Hartley, D. M.; Walsh, D. M.; Ye, C. P. P.; Diehl, T.; Vasquez, S.; Vassilev, P. M.; Teplow, D. B.; Selkoe, D. J. *J. Neurosci.* **1999**, *19*, 8876.
- Bitan, G.; Vollers, S. S.; Teplow, D. B. *J. Biol. Chem.* **2003**, *278*, 34882.
- Kayed, R.; Head, E.; Thompson, J. L.; McIntire, T. M.; Milton, S. C.; Cotman, C. W.; Glabe, C. G. *Science* **2003**, *300*, 486.
- Hardy, J.; Selkoe, D. J. *Science* **2002**, *297*, 353.
- Miravalle, L.; Tokuda, T.; Chiarle, R.; Giaccone, G.; Bugiani, O.; Tagliavini, F.; Frangione, B.; Ghiso, J. *J. Biol. Chem.* **2000**, *275*, 27110.
- Antzutkin, O. N. *Magn. Reson. Chem.* **2004**, *42*, 231.
- Balbach, J.; Ishii, Y.; Antzutkin, O.; Leapman, R.; Rizzo, N.; Dyda, F.; Reed, J.; Tycko, R. *Biochemistry* **2000**, *39*, 13748.
- Ma, B. Y.; Nussinov, R. *Proc. Natl. Acad. Sci. U.S.A.* **2002**, *99*, 14126.
- Klimov, D. K.; Thirumalai, D. *Structure* **2003**, *11*, 295.
- Favrin, G.; Irbach, A.; Mohanty, S. *Biophys. J.* **2004**, *87*, 3657.
- Santini, S.; Mousseau, N.; Derreumaux, P. *J. Am. Chem. Soc.* **2004**, *126*, 11509.
- Wei, G. H.; Mousseau, N.; Derreumaux, P. *Biophys. J.* **2004**, *87*, 3648.
- Santini, S.; Wei, G. H.; Mousseau, N.; Derreumaux, P. *Structure* **2004**, *12*, 1245.
- Cecchini, M.; Rao, F.; Seeber, M.; Caflisch, A. *J. Chem. Phys.* **2004**, *121*, 10748.
- Morimoto, A.; Irie, K.; Murakami, K.; Masuda, Y.; Ohgashi, H.; Nagao, M.; Fukuda, H.; Shimizu, T.; Shirasawa, T. *J. Biol. Chem.* **2004**, *279*, 52781.
- Tjernberg, L. O.; Naslund, J.; Lindqvist, F.; Johansson, J.; Karlstrom, A. R.; Thyberg, J.; Terenius, L.; Nordstedt, C. *J. Biol. Chem.* **1996**, *271*, 8545.
- de la Paz, M. L.; Goldie, K.; Zurdo, J.; Lacroix, E.; Dobson, C. M.; Hoenger, A.; Serrano, L. *Proc. Natl. Acad. Sci. U.S.A.* **2002**, *99*, 16052.
- Garcia, A. E.; Sanbonmatsu, K. Y. *Proteins: Struct., Funct., Genet.* **2001**, *42*, 345.
- Sugita, Y.; Okamoto, Y. *Chem. Phys. Lett.* **1999**, *314*, 141.
- Gnanakaran, S.; Nymeyer, H.; Portman, J.; Sanbonmatsu, K.; Garcia, A. *Curr. Opin. Struct. Biol.* **2003**, *13*, 168.
- Garcia, A.; Sanbonmatsu, K. *Proc. Natl. Acad. Sci. U.S.A.* **2002**, *99*, 2782.
- Nymeyer, H.; Gnanakaran, S.; Garcia, A. E. *Methods Enzymol.* **2004**, *383*, 119.
- Cornell, W. D.; Cieplak, P.; Bayly, C. I.; Gould, I. R.; Merz, K. M.; Ferguson, D. M.; Spellmeyer, D. C.; Fox, T.; Caldwell, J. W.; Kollman, P. A. *J. Am. Chem. Soc.* **1995**, *117*, 5179.
- Jorgensen, W. L.; Chandrasekhar, J.; Madura, J. D.; Impey, R. W.; Klein, M. L. *J. Chem. Phys.* **1983**, *79*, 926.
- Berendsen, H. J. C.; Postma, J. P. M.; Gunsteren, W. F. v.; DiNola, A.; Haak, J. R. *J. Chem. Phys.* **1984**, *81*, 3684.
- Hummer, G.; Soumpasis, D.; Neumann, M. *J. Phys.: Condens. Matter* **1994**, *6*, A141.
- Eker, F.; Griebenow, K.; Schweitzer-Stenner, R. *Biochemistry* **2004**, *43*, 6893.

JA0548337